LATERAL IMPACT OF TUBULAR STRUCTURE – THEORETICAL AND EXPERIMENTAL ANALYSIS. PART 1 – INVESTIGATION OF SINGLE TUBE

Sebastian Lipa

Lodz University of Technology, Institute of Material Science and Engineering, Łódź, Poland

e-mail: sebastian.lipa@p.lodz.pl

Maria Kotełko

Lodz University of Technology, Department of Strength of Materials, Łódź, Poland

e-mail: maria.kotelko@p.lodz.pl

If a thin-walled member is subjected to dynamic load, the estimation of its structural behaviour has to count for the strain-rate influence upon stress-strain material characteristics. It is particularly important when a thin-walled member works as an energy absorber. In the paper, the problem of collapse load, post-failure behaviour and energy dissipation of a tubular structure subjected to lateral impact load is presented. The analytical solution of the problem of initial collapse load and post-failure behaviour of a single tube is discussed. The analysis is limited to the "dynamic progressive crushing", which means that we take into account the strain-rate but neglect inertia effects. The solution is based on the yield-line analysis and takes into account the impact velocity and strain rate, using the Cowper-Symonds constitutive relation. The same problem concerning both the single tube and multi-member tubular structure subjected to lateral bending impact load is solved using Finite Element (FE) simulation, which also takes into account the impact velocity and strain rate, using the corresponding to Cowper-Symonds Perzyna material model. Results of numerical calculations are compared with those obtained from the quasi-dynamic tests performed at different loading velocities on single tubes. The results are shown in load-deformation diagrams and diagrams of deformation patterns.

Key words: tubular structure, lateral bending, impact load, strain rate

1. Introduction

Since demands of general public of safe design of components of vehicles, ships, etc. have increased substantially in the last few decades, a new challenge appeared to design special structural members which would dissipate impact energy in order to limit deceleration and finally to stop a moveable mass (e.g. vehicle) in a controlled manner. Such a structural member termed the energy absorber converts totally or partially kinetic energy into another form of energy. One of the possible design solutions is conversion of kinetic energy of impact into energy of plastic deformation of a thin-walled metallic structural member. A special type of the collapsible energy absorber is a system of moderately thin-walled tubes subject to lateral crushing. Such laterally loaded cylindrical clusters have been used in impact attenuation devices of vehicles. They are also employed as crash cushions in roadside safety applications. Some of these crash cushions are composed of clusters of metallic and non-metallic tubes (Alghamdi, 2001). Another modification of that kind of energy absorbers are tubes (cylinders) stiffened diametrically in order to increase the collapse load without adding weight to the system (Alghamdi, 2001).

A designer of any impact attenuation device must meet two main, sometimes contrary requirements. The initial collapse load must not be too high in order to avoid unacceptably high impact velocities of the vehicle. On the other extreme, the main requirement is a possibly highest

energy dissipation capacity, which may not be achieved if the collapse load of the impact device is too low. The latter may result in dangerously high occupant "ridedown" decelerations (Wu and Carney, 1997).

Different possible configurations of members of the multi-member energy absorber shown in Fig. 1 (number of members, thickness of subsequent tubes, their shape, etc.) allow a designer to fulfil the requirements mentioned above. However, the main advantage of an impact attenuation device formed as a single tube or multi-member cluster of laterally crushed tubes is its load-deformation characteristics, i.e. its collapsing stroke approaching even 95% of the tube original diameter. These unquestionable pros of such energy absorbers are main reasons of great interest in design and research of these devices in recent years.
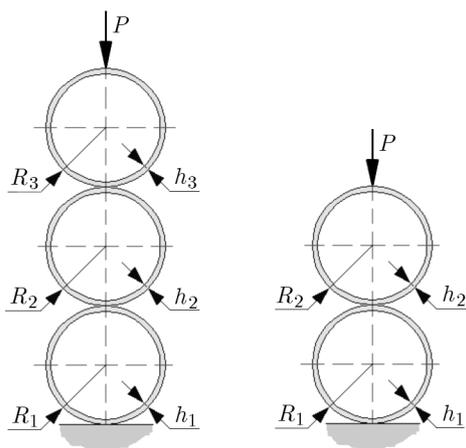

Fig. 1. Alternative lay-out of tubular absorbers

Crushing of a single circular, cylindrical tube between two rigid plates was investigated by De Runtz and Hodge (1963). They carried out experiments and approximate theoretical analysis of the problem, based on the lower-bound approach. Wu and Carney (1997) investigated crushing of single elliptical tubes, both braced (stiffened diametrically) and unbraced, subject to compression between two rigid plates. The analysed theoretically collapse behaviour of the tube using the kinematical method (upper-bound approach) and also the static method (lower-bound approach). They compared analytical results with Finite Element results obtained using ABAQUS software. The same authors compared their theoretical results with the results of experiments (Wu and Carney, 1998).

The works mentioned above were devoted to the analysis of single tubular energy absorbers subjected to lateral crushing load. Both theoretical and experimental analysis of the multi-member tubular absorber subjected to lateral crushing was perfomed by Lipa and Kotełko (Lipa and Kotełko, 2004; Kotełko and Lipa, 2007; Lipa, 2007). If a thin-walled member is subjected to dynamic load, the estimation of its structural behaviour has to count for the strain-rate influence upon stress-strain material characteristics. It is particularly important when a thin-walled member works as an energy absorber. This factor has not been taken into consideration so far in the case of crushing behaviour of the tubular absorbers mentioned above. Thus, within the presented work, the authors discuss the problem of initial crushing load and post-failure behaviour of tubular structure subjected to lateral impact, taking into account in the theoretical analysis the strain rate.

Evaluation of the initial crushing (yield) load of the single tube allows one to determine approximately the corresponding load of the multi-member structure.

Thus, the main aim of the present analysis was to specify and verify simple algorithms of the initial crushing load and post-failure equilibrium path of a single tube, laterally impacted.

Results for a multi-member structure where published previously by Kotełko *et al.* (2009) and Lipa (2007) and are shown below (compared with FE static analysis only).

2. Theoretical model of a laterally loaded circular tube

2.1. Analytical solution

The theoretical model of the single tube subjected to lateral bending is shown in Fig. 2. It is a four-hinge plastic mechanism model used by de Runtz and Hodge (1963) and Lipa and Kotełko (Lipa and Kotełko, 2004; Kotełko and Lipa, 2007; Lipa, 2007).
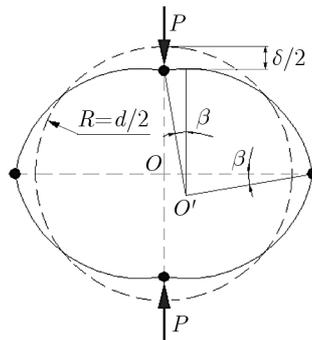

Fig. 2. Four-hinge plastic mechanism model of the single tube

De Runtz and Hodge (1963) obtained the complete lower-bound solution for a thin circular tube subject to lateral crushing between two parallel rigid plates on the assumption of a rigid-perfectly plastic material. They evaluated the initial yield load of the tube using both Huber-von Mises and Tresca yield criteria. The initial yield load is given by the following formula

$$P_0 = \frac{4M_0}{R} \tag{2.1}$$

According to the Huber-von Mises yield criterion $M_0 = \sigma_0 h^2/4$ (where: h – tube thickness; σ_0 – yield stress for static load) is a fully plastic moment at the plastic hinge. De Runtz and Hodge (1963) derived also the load-displacement relation that is as follows

$$P = \frac{P_0}{\sqrt{1 - \left(\frac{\delta}{d}\right)^2}} \tag{2.2}$$

where: δ is the displacement of the load application point; d is the tube diameter.

Using the upper-bound approach, the authors derived an alternative load-displacement relation, starting from the principle of virtual velocities (Kotełko and Lipa, 2007; Lipa, 2007). In that case, the load-displacement relation takes the following form

$$P = 4M_0 \frac{1}{\delta} \arcsin \frac{\delta}{d} \tag{2.3}$$

Both, in relations (2.1) and (2.3), the fully plastic moment M_0 can be expressed in terms of the initial yield stress σ_0, but also by the effective stress $\overline{\sigma}_0$ taking into account the strain hardening effect (Kotełko and Lipa, 2007) and the influence of the strain rate. The hardening effect was investigated by Kotełko and Lipa in previous works. The strain rate effect is discussed in the present paper. The initial yield stress corresponding to the static load is replaced with the initial yield stress under dynamic load, which depends on the strain rate. In the present

solution, the fully plastic moment $M_0 = \sigma_0 h^2/4$ at each plastic hinge is expressed in terms of the plastic flow stress $\overline{\sigma}_0$ depending on strain rate $\dot{\varepsilon}_p$ using the Symonds-Cowper relation

$$\overline{\sigma}_0 = \sigma_0 \Big[1 + \Big(\frac{\dot{\varepsilon}_p}{D}\Big)^{\frac{1}{q}}\Big] \qquad (2.4)$$

where σ_0 is the initial yield stress for static load, $\overline{\sigma}_0$ – initial, plastic flow stress, $\dot{\varepsilon}_p$ – strain rate, q and D – material coefficients.

Additionally, the following assumptions were taken into the analysis:

- The strain-rate $\dot{\varepsilon}_p$, taken into account in (2.4), is of the maximum magnitude, corresponding to the maximum, when the plastic mechanism is entirely developed and takes the final position, i.e. is jammed,

- The maximum strain rate $\dot{\varepsilon}_p$ is calculated on the assumption of the following postulate, which relates the plastic strain ε_p with the angle of rotation β in the following way (Lipa, 2007)

$$\varepsilon_p = \frac{\beta}{2n} \qquad (2.5)$$

where n is a multiple of the beam wall thickness established in the way described by Lipa (2007).

Thus, using postulate (2.5), the maximum value of the strain rate was calculated as follows

$$\dot{\varepsilon}_{p(max)} = \frac{1}{T}\frac{\beta_{lim}}{2n} \qquad (2.6)$$

where T is a time of impact.

Finally, the fully plastic moment, after taking into account the strain rate and hardening effect, takes form

$$M_{0\beta} = \frac{\overline{\sigma}_0 h^2}{4} + \frac{E_t h^2}{12n}\beta \qquad (2.7)$$

where E_t is the tangent modulus (not affected by the strain rate). Relation (2.7) corresponds to the stress distribution in the wall cross-section assumed by Kotełko (2000).

2.2. FE simulation

Numerical FE analysis was performed using commercial software ANSYS version 11 package. In FEM, the model element PLANE 183 was applied. The element formulation is based on logarithmic strain and true stress measures and it is well suited for nonlinear large strain applications. The element allows one to apply different material characteristics taking into account plastic and visco-plastic effects. In the analysis, the bilinear description was applied. The strain rate sensitivity was achieved by application of the Perzyna model, where the coefficients were chosen in accordance to Cowper-Symonds model (2.4), see relation (2.8) (Perzyna, 1963; Perzyna et al., 1971). The visco-plastic Perzyna model applies the isotropic strain hardening, and the integration of constitutive relations is based on repetitive mapping in order to assure compatibility of the tangent stiffness matrix and the stress matrix at the end of each step of integration

$$\dot{\varepsilon} = \gamma\Big(\frac{\sigma}{\sigma_Y} - 1\Big)^{\frac{1}{m}} \qquad (2.8)$$

Relation (2.8) corresponds to Cowper-Symonds relation (2.4), where $\gamma = D$ and $1/m = q$.

In the presented model, the zones of potential contact between compression plate and the specimen (tube) were defined. The contact surface was modeled by means of the elements Targe 169 and Conta 172. The contact problem was solved using the coupling procedure of two surfaces "flexible to flexible" represented by boundary elements of the model. The friction coefficient between two surfaces in contact amounted 0.15 (steel/steel). Figure 3a shows the comparison of load-deformation diagrams obtained from calculations taking into account friction and without friction. As one can notice, the influence of friction is negligible. Figure 3b shows FE simulation of the failure mode – a typical "eight-shape" mode.
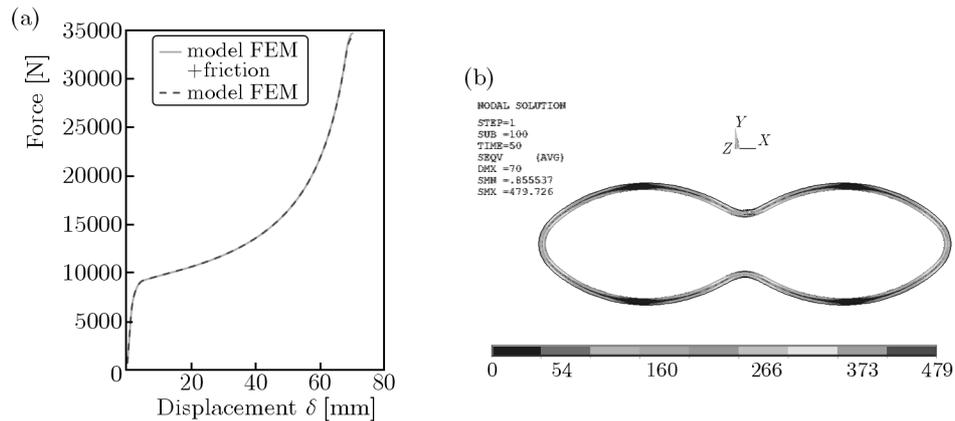
Fig. 3. FE simulations: (a) exemplary load-displacement diagrams, (b) – deformation and the equivalent stress map

In the previous works of the authors, calculations were performed also for multi-member tubular structures of different configurations. The results were presented in Lipa and Kotełko (2004). The analysis was carried out for a static lateral load, and the strain rate was not taken into account.

The aim of this analysis was to search for optimal lay-out of members (sequence of members of different wall thickness). Exemplary load-deformation diagrams are shown in Fig. 4.
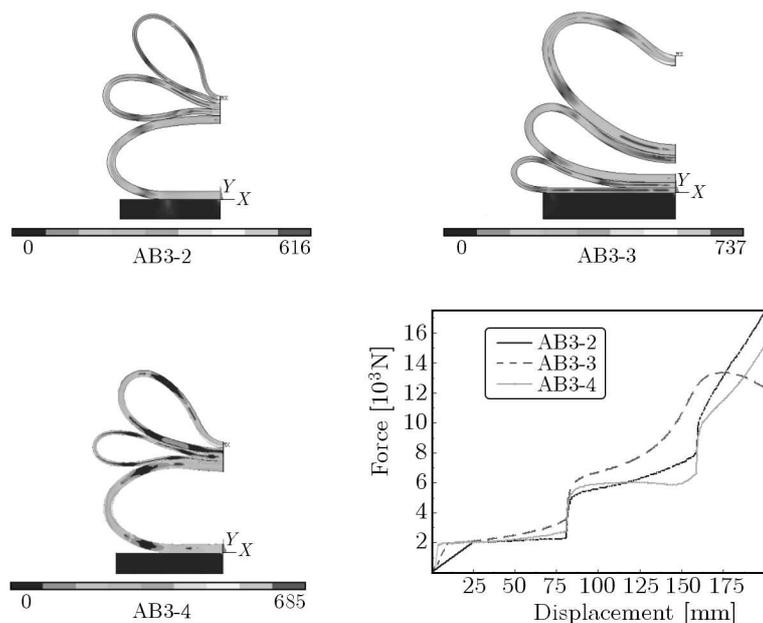

Fig. 4. FE simulation results for multi-member structures of different configurations

Application of a multi-member tubular absorbing structure allows one to raise the amount of energy absorbed the measure of which is the area below the load-deformation curve. As shown in Fig. 4, the subsequent members are included into the crushing process "one by one", and in this way the energy absorbed increases.

3. Experimental verification of theoretrical models – quasi-dynamic tests of single tubes

3.1. Results of experiments

Quasi-dynamic tests have been carried out on short steel tubes subjected to a lateral (radial) force (Fig. 5). Dimensions of specimens and material parameters were as follows:

- tube diameter 88.9 mm; wall thickness $h = 3.2$ mm; tube length 100 mm
- material parameters: yield stress $\sigma_0 = 378$ MPa, tangent modulus $E_t = 500$ MPa, Perzyna (Cowper-Symonds) material coefficients $q = 5$; $D = 40.4$.

The experiment was conducted on the testing machine Instron of loading range 20 kN. Both compressive lateral force and tube radial deformation (displacement of the upper crosshead beam of the testing machine) was recorded using the integrated, computer aided measurement system of the testing machine.
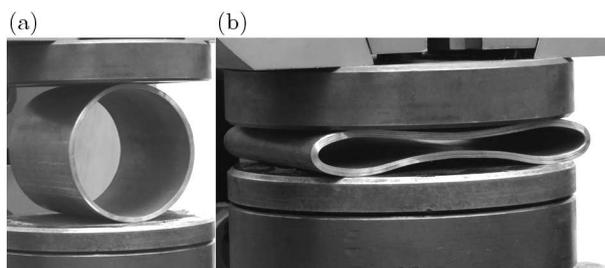

Fig. 5. Compression test of the single tube: (a) – test specimen before loading, (b) – failure mode

The specimens were loaded with different loading velocities, namely: $v_0 = 10, 100, 300, 400$ and 600 mm/min. In Fig. 6, load-shortening experimental diagrams are presented. As is shown, an increase of the initial yield load (maximum load) is not significant, but it should be underlined that the loading velocities applied were low.
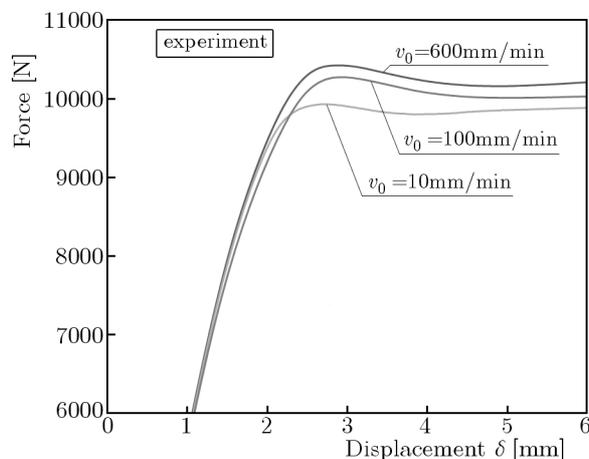

Fig. 6. Compression test diagrams of the single tube for different loading velocities

The results of static tests of multi-member tubular structures were published by Lipa and Kotełko (2004) and Lipa (2007). An exemplary deformation pattern compared with FE simulation is shown in Fig. 7.
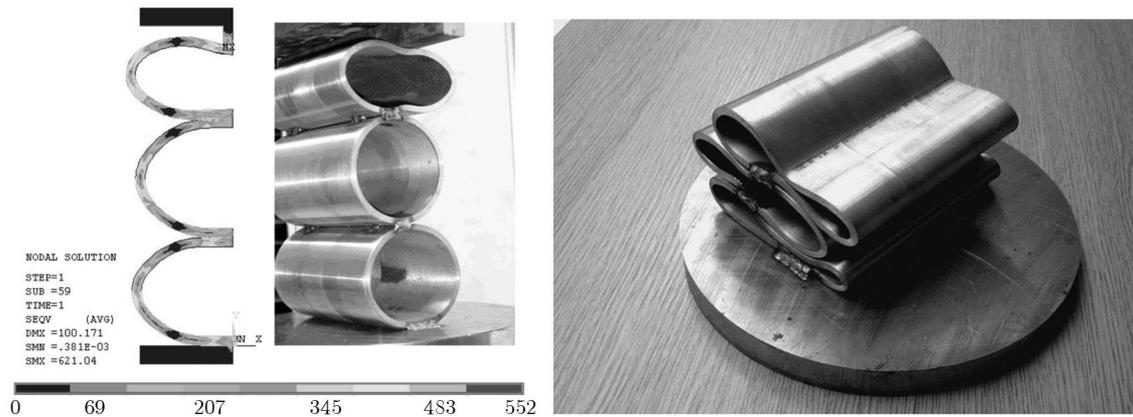

NODAL SOLUTION
STEP=1
SUB =59
TIME=1
SEQV   (AVG)
DMX =100.171
SMN =.381E-03
SMX =621.04

0   69   207   345   483   552

Fig. 7. Comparison of deformation modes (FE simulation and experiment) of the multi-member structure

Also impact tests with the loading velocity 12 m/s were performed by Kotełko and Lippa (2007) on multi-member structures. The results and detailed description of the impact tests were published in Kotełko *et al.* (2009). Exemplary failure patterns are shown in Fig. 8. The dynamic failure pattern is compared with FE simulation for a static loading.

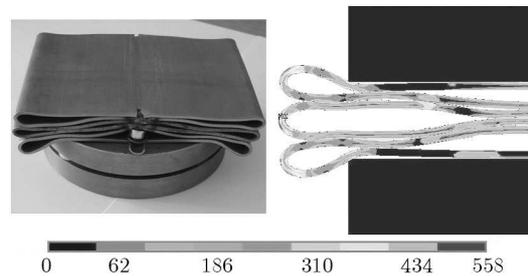0   62   186   310   434   558

Fig. 8. Equivalent stress map and failure mode (comparison of FE simulation and experiment) for the three-member structure

3.2. Comparative study of theoretical and experimental results

The main aim of the present analysis was to specify and verify simple algorithms of the initial crushing load and post-failure equilibrium path of a single tube, laterally impacted. These algorithms are mentioned in Section 2.1. Figure 9 shows the comparison of the failure mode of a single steel tube laterally loaded with the velocity $v_0 = 600$ mm/min and deformation pattern obtained from FE simulation.

In Fig. 10, load-deformation diagrams are presented, obtained using de Runtz and Hodge algorithm (2.3), upper-bound estimation (kinematic model) (2.4) and the experimental curve for the loading velocity $v_0 = 600$ mm/min. The better agreement of the theory and experiment is achieved for de Runtz and Hodge algorithm. In both theoretical algorithms, the strain-rate effect is taken into account. Figure 11 shows the comparison of FE theoretical and experimental load-deformation paths for a single tube under lateral compression, namely, the FE curve based on the Perzyna material model and experimental verification for the loading velocity $v_0 = 600$ mm/min.

In Fig. 12a, the influence of the strain-rate in the analytical solution based on de Runtz and Hodge algorithm is presented. The curve taking into account the strain-rate is in much better
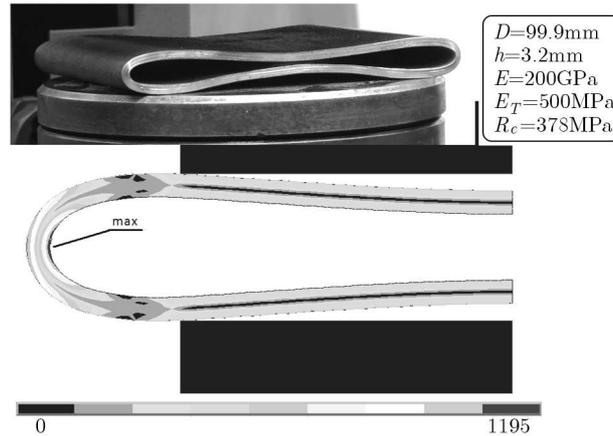
Fig. 9. Failure mode of the tested specimen and its FE simulation
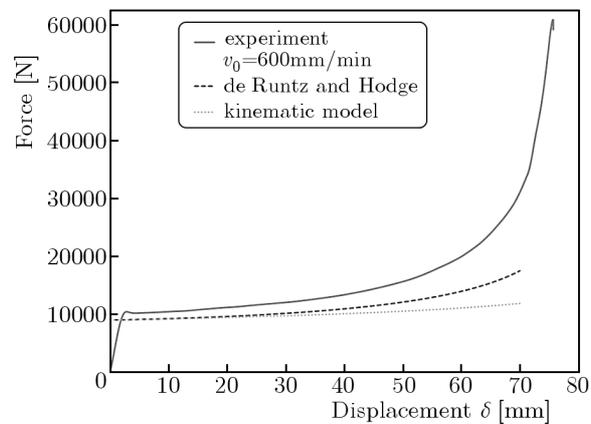

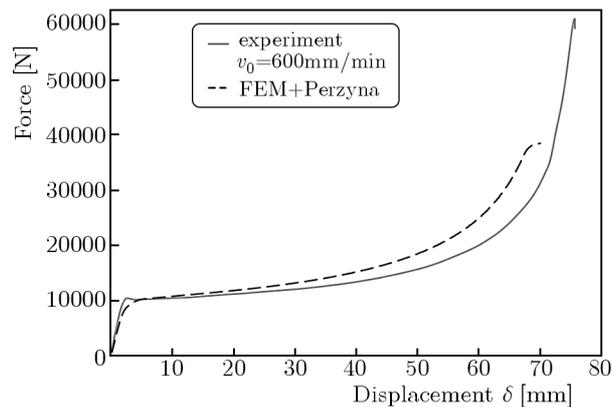Fig. 10. Comparison of the experimental results with analytical solutions

Fig. 11. Comparison of the experimental results with theoretical FE simulation

agreement with the experimental results. Figure 12b shows the load-displacement diagrams obtained from the experimental tests and FE calculations. Surprising is that the FE curve (indicated as "FEM model"), which does not take into account the strain-rate, is above the curve based on the Perzyna material model in the plastic range (plastic plateau and final stage of failure). However, the initial crushing load is higher when taking into account the strain-rate (Perzyna model).
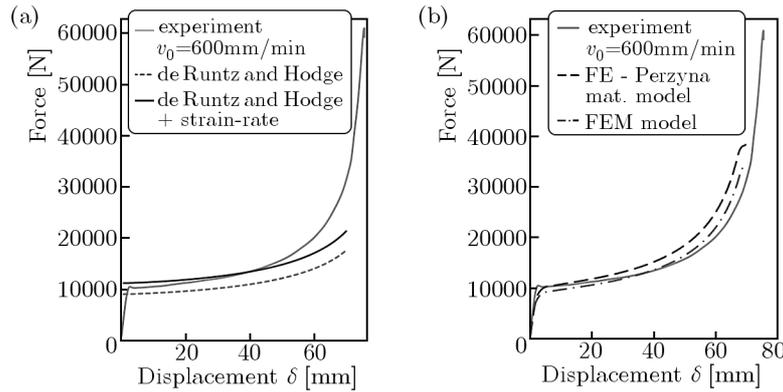
Fig. 12. Exemplary comparative load-displacemnt diagrams: (a) – comparison of the analytical solution and experiment, (b) – comparison of the FE results and experiment

4. Conclusions

As was mentioned in the introduction, the main aim of the present analysis was to specify and verify simple algorithms of the initial crushing load and post-failure equilibrium path of a single tube, laterally impacted. The verification was performed in two ways: using the numerical FE "experiment" and the quasi-dynamic tests performed on the testing machine.

Generaly, a very good agreement of the FE simulations and experimental results was achieved. However, the results obtained from the kinematical approach (single tube – upper-bound estimation) are underestimated in comparison with the experiment and FE simulations. A satisfactory agreement was obtained between the theoretical initial crushing load for the single tube calculated using the improved de Runtz and Hodge algorithm (lower-bound) taking into account strain rate and FE simulations as well as experimental results. Thus, this simple analytically based algorithm can be applied for preliminary estimation of the initial crushing load and post-failure response of the single tube subjected to lateral impact. Such an algorithm is useful in the initial stage of the absorber design process.

The improved de Runtz and Hodge algorithm can also be applied for the preliminary estimation of the multi-member tubular absorber response to the impact lateral load. A proposal of the approximate algorithm was given by Lipa (2007).

Further investigation should be carried out in two areas: firstly – both theoretical calculations (based on the improved de Runtz and Hodge algorithm and FE simulations) have to be performed for higher loading (impact) velocities and compared with results of experimental impact tests. Secondly, FE simulations taking into account the strain-rate should be extended onto multi-member structures and also compared with results of impact tests of such structures. Then, applicability of the improved de Runtz and Hodge algorithm for a single tube and approximate calculation of a multi-member structure subjected to impact load can be proved. Results of these investigations are planned to be published by the authors in Part II (a paper devoted to the multi-member structure).

References

1. ALGHAMDI A.A.A., 2001, Collapsible impact energy absorbers: an overview, *Thin-Walled Structures*, **39**, 189-213

2. DE RUNTZ J.A., HODGE P.G., 1963, Crushing of a tube between rigid plates, *Journal of Applied Mechanics*, **30**, 391-395

3. KOTEŁKO M., 2000, Damage mechanisms of thin-walled girders under bending with iso- and orthotropic walls (in Polish), *Scientific Bulletin of Lodz University of Technology*, **844**, *ser. Transactions*, **273**

4. KOTEŁKO M., LIPA S., 2007, Crushing of tubular multi-member absorbers under lateral compression – experimental verification of theoretical algorithm, *24th DANUBIAADRIA Symposium on Advances in Experimental Mechanics*, Romania

5. KOTEŁKO M., LIPA S., MANIA R.J., 2009, Dynamic crushing tests of thin-walled members under compression, *Materials Engineering*, **16**, 1, 14-19

6. LIPA S., 2007, Analysis of dissipation properties of energy absorbers made of thin-walled tubes subject to crushing (in Polish), Ph.D. Thesis, Poland, Lodz University of Technology

7. LIPA S., KOTEŁKO M., 2004, Numerical and experimental collapse analysis of tubular multi-member energy absorbers under lateral compression, *Journal of Theoretical and Applied Mechanics*, **42**, 4, 842-857

8. PERZYNA P., 1963, The study of the dynamic behavior of rate sensitive plastic materials, *Archive of Applied Mechanics*, **15**, 1, 113-129

9. PERZYNA P., KLEPACZKO J., BEJADA J., 1971, *Application of Visco-Elesticity*, Ossolineum

10. WU L., CARNEY J.F., 1997, Initial collapse of braced elliptical tubes under lateral compression, *International Journal of Mechanical Sciences*, **39**, 9, 1023-1036

11. WU L., CARNEY III J.F., 1998, Experimental analysis of collapse behaviour of braced elliptical tubes under lateral compression, *International Journal of Mechanical Sciences*, **40**, 8, 761-777